Inorg. Chem. **2007**, *46*, 4548–4559

Tuning the Selectivity/Specificity of Fluorescent Metal Ion Sensors Based on N_2S_2 Pyridine-Containing Macrocyclic Ligands by Changing the Fluorogenic Subunit: Spectrofluorimetric and Metal Ion Binding Studies

M. Carla Aragoni,[†] Massimiliano Arca,[†] Andrea Bencini,[‡] Alexander J. Blake,[#] Claudia Caltagirone,[†] Greta De Filippo,[†] Francesco A. Devillanova,[†] Alessandra Garau,[†] Thomas Gelbrich,[§] Michael B. Hursthouse,[§] Francesco Isaia,[†] Vito Lippolis,*[,†] Marta Mameli,[†] Palma Mariani,[‡] Barbara Valtancoli,[‡] and Claire Wilson[#]

Dipartimento di Chimica Inorganica ed Analitica, Università degli Studi di Cagliari, S.S. 554 Bivio per Sestu, 09042 Monserrato, Italy, Dipartimento di Chimica, Università di Firenze, Polo Scientifico, Via della Lastruccia 3, 50019 Sesto Fiorentino, Florence, Italy, School of Chemistry, The University of Nottingham, University Park, Nottingham NG7 2RD, U.K., and Department of Chemistry, The University of Southampton, Highfield, Southampton SO17 1BJ, U.K.

Received January 30, 2007

Two new fluorescent chemosensors for metal ions have been synthesized and characterized, and their photophysical properties have been explored; they are the macrocycles 5-(2-quinolinylmethyl)-2,8-dithia-5-aza-2,6-pyridinophane (**L**^{5}) and 5-(5-chloro-8-hydroxyquinolinylmethyl)-2,8-dithia-5-aza-2,6-pyridinophane (**L**^{6}). Both systems have a pyridyl-thioether-containing 12-membered macrocycle as a binding site. The coordination properties of these two ligands toward Cu^{II}, Zn^{II}, Cd^{II}, Hg^{II}, and Pb^{II} have been studied in MeCN/H_2O (1:1 v/v) and MeCN solutions and in the solid state. The stoichiometry of the species formed at 25 °C have been determined from absorption, fluorescence, and potentiometric titrations. The complexes [Cu**L**^{5}]$(ClO_4)_2$·$^1/_2$MeCN, [Zn**L**^{5}(H_2O)]$(ClO_4)_2$, [Hg**L**^{5}(MeCN)]$(ClO_4)_2$, [Pb**L**^{5}-$(ClO_4)_2$], [Cu_3(5-Cl-8-HDQH$_{-1}$)(**L**^{6}H$_{-1}$)$_2$]$(ClO_4)_3$·7.5H_2O (HDQ = hydroxyquinoline), and [Cu(**L**^{6})$_2$]$(BF_4)_2$·2$MeNO_2$ have also been characterized by X-ray crystallography. A specific CHEF-type response of **L**^{5} and **L**^{6} to the presence of Zn^{II} and Cd^{II}, respectively, has been observed at about pH 7.0 in MeCN/H_2O (1:1 v/v) solutions.

Introduction

The development of artificial chemosensors, discrete molecules that selectively recognize and signal to an external operator the presence of a specific analyte in a complex matrix, is one of the main achievements of supramolecular chemistry and a vigorous research area. The intense interest in this field is driven by the growing demand for extremely sensitive and selective analytical tools for the detection and monitoring of charged and neutral substrates in biological, environmental, and industrial waste effluent samples. In this respect, fluorescent chemosensors are of particular importance because they offer the advantage of high sensitivity and require relatively simple signal-detection techniques.[1−21] From a structural point of view, these compounds can be classified into two main classes: *intrinsic* chemosensors, in which both functions of recognizing and signaling a given analyte are performed by a fluorophore, and *conjugated*

* To whom correspondence should be addressed. E-mail: lippolis@unica.it. Phone: +39 070 6754467. Fax: +39 070 6754456.
[†] Università degli Studi di Cagliari.
[‡] Università di Firenze.
[#] The University of Nottingham.
[§] The University of Southampton.

(1) de Silva, A. P.; Gunaratne, H. Q. G.; Gunnlaugsson, T.; Huxley, A. J. M.; McCoy, C. P.; Rademacher, J. T.; Rice, T. E. *Chem. Rev.* **1997**, *97*, 1515.
(2) *Chemosensors of Ions and Molecular Recognition*; Czarnik, A. W., Desvergene, J.-P., Eds.; NATO ASI Series C; Kluwer Academic Publishers: Dordrecht, The Netherlands, 1997; Vol. 492.
(3) Kimura, E.; Koike, T. *Chem. Soc. Rev.* **1998**, *27*, 179.
(4) (a) Valeur, B.; Leray, I. *Coord. Chem. Rev.* **2000**, *205*, 3. (b) Métivier, R.; Leray, I.; Valeur, B. *Chem. Commun.* **2003**, 996.
(5) Balzani, V.; Cerioni, P.; Gestermann, S.; Kauffmann, C.; Gorka, M.; Vögtle, F. *Chem. Commun.* **2000**, 853.
(6) (a) Prodi, L.; Bolletta, F.; Montalti, M.; Zaccheroni, N. *Coord. Chem. Rev.* **2000**, *205*, 59. (b) Prodi, L. *New. J. Chem.* **2005**, *29*, 20.
(7) Rurack, K. *Spectrochim. Acta, Part A* **2001**, *57*, 2161.
(8) Parack, K.; Resch-Genger, U. *Chem. Soc. Rev.* **2002**, *31*, 116.
(9) Fabbrizzi, L.; Licchelli, M.; Taglietti, A. *Dalton Trans.* **2003**, 3471.

10.1021/ic070169e CCC: $37.00
Published on Web 04/18/2007

Scheme 1. Summary of Fluorescent Chemosensors Based on $\mathbf{L^1}$

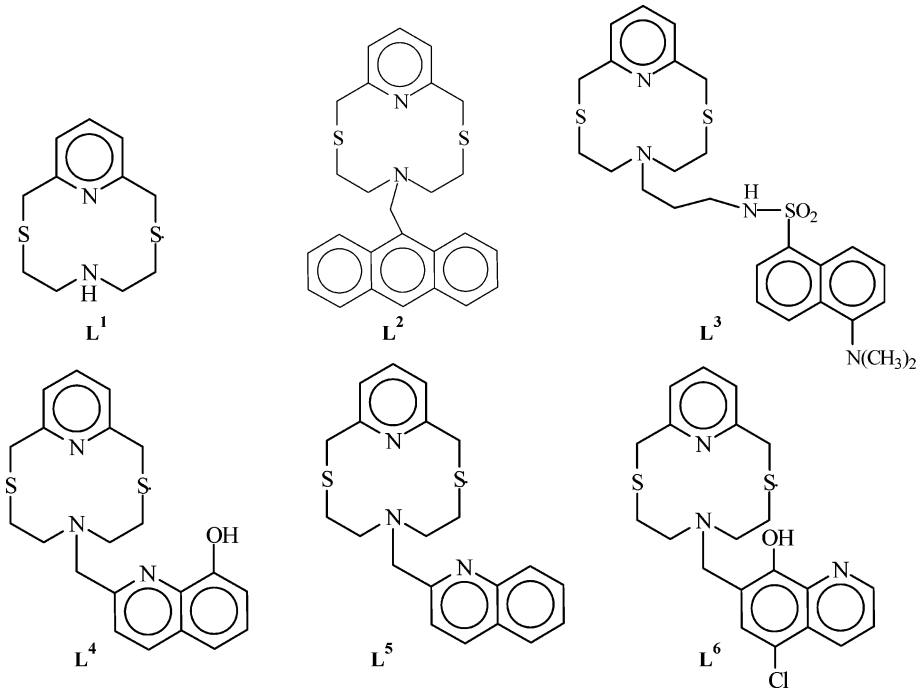

chemosensors, which consist of a fluorogenic fragment (signaling unit) covalently linked, through an appropriate spacer, to a guest-binding site (receptor unit). The latter class of chemosensors is the most common and studied; the selective host−guest interaction of the target species with the receptor unit (recognition event) is converted into an optical signal expressed as an enhancement or quenching of the fluorophore emission. According to this simple "receptor−spacer−fluorophore" supramolecular modular scheme, the selectivity/specificity of conjugated chemosensors would be determined solely or mainly by the nature of the receptor unit, while the transduction mechanism that is triggered upon the host−guest interaction and the sensitivity or sensor performance would be determined mainly by the fluorogenic fragment. This subdivision of the roles played by the receptor and fluorescent signaling units, which can be translated into the operative synthetic strategy "find the appropriate receptor and attach to it a fluorogenic fragment", although very simplistic, certainly represents a useful guide to the design of a conjugated fluorescent chemosensor, and it has worked very well for metal cation sensors featuring anthracenyl derivatives of crown ethers.[1] However, the choice of the "read-out" or signaling unit can be critical to both the performance and the selectivity/specificity of the sensor, especially if a direct interaction of the fluorophore with the target species is implied. In this respect, the complementary approach of changing the signaling unit attached to a predefined receptor unit (not necessarily the best in the binding process) could therefore represent a promising alternative to the common practice in the design of specific and selective conjugated fluorescent chemosensors of using different receptors linked to the same fluorophore.[1−9,21b,c]

Very recently, as part of a research program to study both the coordination chemistry of mixed thia-aza macrocycles containing heteroaryl fragments and their analytical applications as selective ionophores toward heavy and transition metal ions,[22−25] we have described the coordination properties of the new pyridine-based N_2S_2-donating 12-membered macrocycle 2,8-dithia-5-aza-2,6-pyridinophane ($\mathbf{L^1}$).[26] The *N*-(9-anthracenyl)methyl ($\mathbf{L^2}$), *N*-dansylamidopropyl ($\mathbf{L^3}$),

(10) Zao, J.; Davidson, M. G.; Mahon, M. F.; Kociok-Köhn, G.; James, T. D. *J. Am. Chem. Soc.* **2004**, *126*, 16179.
(11) Fernandez, Y. D.; Pérez Gramatges, A.; Amendola, V.; Foti, F.; Mangano, C.; Pallavicini, P.; Patroni, S. *Chem. Commun.* **2004**, 1650.
(12) Pohl, R.; Aldakov, D.; Kubát, P.; Jursíková, K.; Marquez, M., Jr.; Anzenbacher, P. *Chem. Commun.* **2004**, 1282.
(13) Zheng, Y.; Orbelescu, J.; Ji, X.; Andreopoulos, F. M.; Pham, S. M.; Leblanc, R. M. *J. Am. Chem. Soc.* **2003**, *125*, 2680.
(14) Yang, W.; Yan, J.; Fang, H.; Wang, B. *Chem. Commun.* **2003**, 792.
(15) Kaletas, B. K.; Williams, R. M.; König, B.; De Cola, L. *Chem. Commun.* **2002**, 776.
(16) Nolan, E. M.; Burdette, S. C.; Harvey, J. H.; Hildebrand, S. A.; Lippard, S. J. *Inorg. Chem.* **2004**, *43*, 2624.
(17) Special Issue on Fluorescent Sensors. *J. Mater. Chem.* **2005**, *15*, 2617−2976.
(18) Amendola, A.; Fabbrizzi, L.; Foti, F.; Licchelli, M.; Mangano, C.; Pallavicini, P.; Poggi, A.; Sacchi, D.; Taglietti, A. *Coord. Chem. Rev.* **2006**, *250*, 273.
(19) Goldsmith, C. R.; Lippard, S. J. *Inorg. Chem.* **2006**, *45*, 555.
(20) (a) Song, K. C.; Kim, J. S.; Park, S. M.; Chung, K.-C.; Ahn, S.; Chang, S.-K. *Org. Lett.* **2006**, *8*, 3413. (b) Wu, Z.; Zhang, Y.; Ma, J. S.; Yang, G. *Inorg. Chem.* **2006**, *45*, 3140.
(21) (a) Lim, N. C.; Schuster, J. V.; Porto, M. C.; Tanudra, M. A.; Yao, L.; Freake, H. C.; Brückener, C. *Inorg. Chem.* **2005**, *44*, 2018. (b) Yoon, S.; Albers, A. E.; Wong, A. P.; Chang, C. J. *J. Am. Chem. Soc.* **2005**, *127*, 16030. (c) He, Q.; Miller, E. W.; Wong, A. P.; Chang, C. J. *J. Am. Chem. Soc.* **2006**, *128*, 9316.
(22) Aragoni, M. C.; Arca, M.; Demartin, F.; Devillanova, F. A.; Isaia, F.; Garau, A.; Lippolis, V.; Papke, U.; Shamsipur, M.; Tei, L.; Yari, A.; Verani, G. *Inorg. Chem.* **2002**, *41*, 6623.
(23) (a) Caltagirone, C.; Bencini, A.; Demartin, F.; Devillanova, F. A.; Garau, A.; Isaia, F.; Lippolis, V.; Papke, U.; Tei, L.; Verani, G. *Dalton Trans.* **2003**, 901. (b) Tei, L.; Blake, A. J.; Cooke, P. A.; Caltagirone, C.; Demartin, F.; Lippolis, V.; Morale, F.; Wilson, C.; Schröder, M. *J. Chem. Soc., Dalton Trans.* **2002**, 1662. (c) Arca, M.; Blake, A. J.; Lippolis, V.; Montesu, D. R.; McMaster, J.; Tei, L.; Schröder, M. *Eur. J. Inorg. Chem.* **2003**, 1232.
(24) Aragoni, M. C.; Arca, M.; Bencini, A.; Blake, A. J.; Caltagirone, C.; Decortes, A.; Demartin, F.; Devillanova, F. A.; Faggi, E.; Dolci, L. S.; Garau, A.; Isaia, F.; Lippolis, V.; Prodi, L.; Wilson, C.; Valtancoli, B.; Zaccheroni, N. *Dalton Trans.* **2005**, 2994.

and *N*-(8-hydroxy-2-quinolinyl)methyl (**L**^{4}) pendent arm derivatives of **L**^{1} were also synthesized, and their optical response to the metal ions Cu^{II}, Zn^{II}, Cd^{II}, Hg^{II}, and Pb^{II} was investigated in MeCN/H_2O (4:1 v/v) solutions.[26] Contrary to expectation, the presence of S-donors in the macrocyclic framework did not confer on **L**^{2}−**L**^{4} a specific and selective change in the fluorescent emission upon interaction with the "borderline" and "soft" metal ions considered. This was particularly evident in the case of **L**^{2} where the anthracenyl moiety does not participate in the complexation process.[26] However, for **L**^{3} and **L**^{4}, the presence of coordinatively active fluorogenic fragments influenced the specificity of the guest binding event: the former ligand responded in terms of changes of fluorescence emission only to the presence of Hg^{II} or Cu^{II}, and the latter ligand responded only to the presence of Zn^{II} or Cd^{II}. Following these results, we report the synthesis, coordination properties, and optical responses to the above-mentioned metal ions in MeCN/H_2O (1:1 v/v) and MeCN solutions of two new derivatives of **L**^{1} bearing the 2-quinolinylmethyl (**L**^{5}) and 5-chloro-8-hydroxyquinolinylmethyl (**L**^{6}) pendent arms. The optical properties of **L**^{5} and **L**^{6} in the presence of metal ions are compared with those of **L**^{2}−**L**^{4},[26] and they illustrate the potential of the complementary strategy of linking different fluorophores to the same receptor unit, in the design of specific and selective conjugated fluorescent chemosensors.

Experimental Section

Instruments and Materials. Microanalytical data were obtained using a Fisons EA CHNS−O instrument (T = 1000 °C). ^{13}C and ^{1}H NMR spectra were recorded on a Varian VXR300 spectrometer (operating at 299.92 MHz). The ESI mass spectra were recorded using a Bruker MicroTof mass spectrometer. The spectrophotometric measurements were carried out at 25 °C using a Varian model Cary 5 UV−vis NIR spectrophotometer and a Thermo Nicolet Evolution 300 spectrophotometer. Uncorrected emission spectra were obtained with a Varian Cary Eclipse fluorescence spectrophotometer. To allow comparison among the emission intensities, we performed corrections for instrumental response, inner-filter effect, and phototube sensitivity.[27] A correction for differences in the refractive index was introduced when necessary. Luminescence quantum yields (uncertainty of ±15%) were determined using quinine sulfate in a 1 M H_2SO_4 aqueous solution (Φ = 0.546) as a reference. For spectrophotometer measurements, MeCN (Uvasol, Merck) and Millipore grade water were used as solvents. Spectrofluorimetric titrations of the **L**^{5} and **L**^{6} with metal ions were performed by the addition of increasing volumes of a solution of the metal ion to a solution of the ligand (3 mL), buffered at pH 7.0 with HEPES (1 M, 3 μL, H_2O solution) [4-(2-hydroxyethyl)piperazine-1-ethanesulfonic acid]. Solutions of the ligands in MeCN/H_2O (1:1 v/v) were 2.5×10^{-5} M, and those of the metals in H_2O were 2.5×10^{-3} M. Spectrofluorimetric titrations at variable pHs of **L**^{5} and **L**^{6} were instead performed by the addition of increasing volumes of 0.5 M aqueous NaOH to an acid solution of the ligand or its 1:1 metal ion complex in MeCN/H_2O (1:1 v/v,-10 mL, 2.5×10^{-5} M) in the presence of HEPES 1 M (100 μL, H_2O solution); the initial pH was adjusted by the addition of aqueous HCl (0.2 mL, 0.5 M). In all cases, the effect of dilution on fluorescence emission was neglected. Solvents for other purposes and starting materials [2-(chloromethyl)quinoline) and 5-chloro-8-hydroxyquinoline (5-Cl-8-HDQ)] were purchased from commercial sources where available. The macrocyclic ligand 2,8-dithia-5-aza-2,6-pyridinophane (**L**^{1}) was synthesized according to the reported procedure.[26]

Caution! Most of the reported metal complexes with **L**^{5} and **L**^{6} were isolated in the solid state as perchlorate salts. We have worked with these complexes on a small scale without any incident. Despite these observation, the unpredictable behavior of perchlorate salts necessitates extreme care in handling.

Synthesis of 5-(2-Quinolinylmethyl)-2,8-dithia-5-aza-2,6-pyridinophane (L^{5}). A solution of 2-(chloromethyl)quinoline (0.18 g, 0.84 mmol) in dry MeCN (15 mL) was added dropwise to a mixture of **L**^{1} (0.2 g, 0.83 mmol) and K_2CO_3 (0.57 g, 4.15 mmol) in dry MeCN (20 mL). The mixture was heated to reflux for 24 h under nitrogen. The solid was filtered off, and the solvent was removed under reduced pressure. The residue was dissolved in CH_2Cl_2 and washed with water. The organic phase was dried over Na_2SO_4, and the solvent was removed under reduced pressure. The resulting brown oil was purified by flash chromatography (silica) using CH_2Cl_2/MeOH (10/0.5 v/v) as the eluant to give a pale yellow solid (0.16 g, 50.5%). mp: 124−126 °C. Anal. Found (Calcd) for $C_{21}H_{23}N_3S_2$: C, 66.13 (66.11); H, 6.06 (6.08); N, 11.00 (11.01); S, 16.85 (16.81%). ^{1}H NMR (300 MHz, $CDCl_3$): δ_H 2.56 (br s 8H, SCH_2CH_2N), 3.80 (s, 4H, ArCH_2S), 3.88 (s, 2H, NCH_2Ar), 7.28 (d, J = 7.8 Hz, 2H), 7.41−7.52 (m, 1H), 7.55 (d, J = 8.7 Hz, 1H), 7.60−7.80 (m, 3H), 7.97 (d, J = 8.1 Hz, 1H), 8.05 (d, J = 8.7 Hz, 1H). ^{13}C NMR (300 MHz, $CDCl_3$): δ_c 25.15 (S*C*H_2CH$_2$N), 36.53 (Ar*C*H$_2$S), 51.33 (SCH$_2$*C*H$_2$N), 60.70 (N*C*H$_2$Ar), 120.33 (Q), 121.45 (Py), 125.87 (Q), 127.16 (Q), 127.28 (Q), 128.72 (Q), 129.12 (Q), 136.15 (Q), 137.98 (Py), 147.24 (Q), 157.39 (Py), 160.23 (Q) [Py = pyridine framework, Q = quinoline framework]. UV−vis: (MeCN, 25 °C) λ_{max} (ϵ_{max}) 209 (47 000), 270 (7500), 315 nm (2700 dm^3 mol^{-1} cm^{-1}); (MeCN/H_2O 1:1 v/v, 25 °C) λ_{max} (ϵ_{max}) 227 (39 100), 273 (8000), 302 (3600), 316 nm (4000 dm^3 mol^{-1} cm^{-1}). MS (ES+): m/z 381 ([**L**^{5}]$^{+}$).

Synthesis of 5-(5-Chloro-8-hydroxyquinolinylmethyl)-2,8-dithia-5-aza-2,6-pyridinophane (L^{6}). 5-Chloro-8-hydroxyquinoline (0.27 g, 1.59 mmol) and paraformaldehyde (0.12 g, 4.00 mmol) were added to a mixture of **L**^{1} (0.3 g, 1.25 mmol) in dry benzene (50 mL). The solution was heated to reflux for 12 h under nitrogen. The solvent was evaporated under reduced pressure, and the residue was washed with Et_2O to give a yellow solid (0.25 g, yield 46.3%). mp: 125 °C. Anal. Found (calcd) for $C_{21}H_{22}ClN_3OS_2$: C, 58.38 (58.39); H, 5.15 (5.13); N, 9.75 (9.73); S, 14.83 (14.84%). ^{1}H NMR (300 MHz, $CDCl_3$): δ_H 2.57 (br s, 8H, SCH_2CH_2N), 3.76 (s, 4H, ArCH_2S), 3.78 (s, 2H, NCH_2Ar), 7.24 (d, J = 8.0 Hz, 2H), 7.31−7.52 (m, 2H), 7.64 (t, J = 8.0 Hz, 1H), 8.36 (d, J = 8.4 Hz, 1H), 8.79 (d, J = 8.4 Hz, 1H). ^{13}C NMR (300 MHz, $CDCl_3$): δ_c 24.66 (Ar*C*H$_2$S), 36.56 (S*C*H$_2$CH$_2$N), 50.77 (NCH$_2$Ar), 54.81 (NCH$_2$-Ar), 119.96 (*C*−Cl, Q), 121.60 (Py), 121.87 (Q), 122.40 (Q), 125.76 (Q), 127.24 (Q), 132.68 (Q), 138.25 (Py), 139.27 (*C*−OH, Q),

(25) (a) Shamsipur, M.; Javanbakht, M.; Mousavi, M. F.; Ganjali, M. R.; Lippolis, V.; Garau, A.; Tei, L. *Talanta* **2001**, *55*, 1047. (b) Shamsipur, M.; Javanbakht, M.; Lippolis, V.; Garau, A.; De Filippo, G.; Ganjali, M. R.; Yari, A. *Anal. Chim. Acta* **2002**, *462*, 225. (c) Shamsipur, M.; Javanbakht, M.; Ganjali, M. R.; Mousavi, M. F.; Lippolis, V.; Garau, A. *Electroanalysis* **2002**, *14*, 1691. (d) Shamsipur, M.; Poursaberi, T.; Rezapour, M.; Ganjali, M. R.; Mousavi, M. F.; Lippolis, V.; Montesu, D. R. *Electroanalysis* **2004**, *16*, 1336. (e) Shamsipur, M.; Hosseini, M.; Alizadeh, K.; Alizadeh, N.; Yari, A.; Caltagirone, C.; Lippolis, V. *Anal. Chim. Acta* **2005**, *533*, 17. (f) Shamsipur, M.; Hosseini, M.; Alizadeh, K.; Mousavi, M. F.; Garau, A.; Lippolis, V.; Yari, A. *Anal. Chem.* **2005**, *77*, 276.
(26) Blake, A. J.; Bencini, A.; Caltagirone, C.; De Filippo, G.; Dolci, L. S.; Garau, A.; Isaia, F.; Lippolis, V.; Mariani, P.; Prodi, L.; Montalti, M.; Zaccheroni, N.; Wilson, C. *Dalton Trans.* **2004**, 2771.
(27) Credi, A.; Prodi, L. *Spectrochim. Acta* **1998**, *54*, 159.

Table 1. Crystallographic Data for $[Cu\mathbf{L}^5](ClO_4)_2 \cdot {}^1/_2MeCN$, $[Zn\mathbf{L}^5(H_2O)](ClO_4)_2$, $[Hg\mathbf{L}^5(MeCN)](ClO_4)_2$, $[Pb\mathbf{L}^5(ClO_4)_2]$, $[Cu_3(5\text{-Cl-8-HDQH}_{-1})(\mathbf{L}^6H_{-1})_2](ClO_4)_3 \cdot 7.5H_2O$, and $[Cu(\mathbf{L}^6)_2](BF_4)_2 \cdot 2MeNO_2$

	$[Cu\mathbf{L}^5](ClO_4)_2 \cdot {}^1/_2MeCN$	$[Zn\mathbf{L}^5(H_2O)](ClO_4)_2$	$[Hg\mathbf{L}^5(MeCN)](ClO_4)_2$	$[Pb\mathbf{L}^5(ClO_4)_2]$	$[Cu_3(5\text{-Cl-8-HDQH}_{-1})(\mathbf{L}^6H_{-1})_2](ClO_4)_3 \cdot 7.5H_2O$	$[Cu(\mathbf{L}^6)_2](BF_4)_2 \cdot 2MeNO_2$
formula	$C_{22}H_{24.5}Cl_2CuN_{3.5}O_8S_2$	$C_{21}H_{25}Cl_2N_3O_9S_2Zn$	$C_{23}H_{26}Cl_2HgN_4O_8S_2$	$C_{21}H_{23}Cl_2N_3O_8PbS_2$	$C_{51}H_{62}Cl_6Cu_3N_7O_{22.5}S_4$	$C_{44}H_{50}B_2Cl_2CuF_8N_8O_6S_4$
M (g mol^{-1})	664.51	663.83	822.09	787.63	1664.64	1223.22
cryst syst	monoclinic	monoclinic	monoclinic	monoclinic	triclinic	monoclinic
space group	$P2_1$ (No. 4)	$P2_1/c$ (No. 14)	$I2/a$ (No. 15)	$P2_1/n$ (No.14)	$P\bar{1}$ (No. 2)	$P2_1/c$ (No. 14)
a (Å)	11.8164(12)	12.3734(10)	22.199(2)	9.4031(8)	12.297(3)	6.7570(17)
b (Å)	14.494(2)	14.1375(12)	8.7307(5)	20.719(2)	17.199(4)	25.205(6)
c (Å)	15.890(2)	14.9149(12)	28.982(2)	12.8426(11)	17.234(4)	15.048(4)
α (deg)					116.069(4)	
β (deg)	108.924(2)	96.326(1)	98.407(2)	90.956(2)	104.143(4)	100.38(2)
γ (deg)					91.725(4)	
U (Å^3)	2574.3(8)	2593.2(4)	5556.7(7)	2501.7(4)	3135.1(13)	2520.9(11)
Z	4	4	8	4	2	2
T (K)	150(2)	150(2)	150(2)	150(2)	150(2)	120(2)
D_c (g cm^{-3})	1.715	1.700	1.965	2.091	1.763	1.611
μ (mm^{-1})	1.274	1.371	5.937	7.178	1.482	0.792
unique reflns (R_{int})	9034 (0.017)	5927 (0.0215)	6363 (0.099)	5623 (0.026)	8960 (0.124)	4750, 0.136
obsd reflns	8278 [$I > 2\sigma(I)$]	5671	5723	4761	4114	3022
abs correction	multiscan[30]	multiscan[30]	multiscan[31]	multiscan[30]	multiscan[31]	multiscan[32]
T_{max}, T_{min}	1.00, 0.867	0.850, 0.722	0.140, 0.060	0.560, 0.258	0.965, 0.743	0.992, 0.858
R1, wR2 (all data)	0.0412, 0.0960	0.0400, 0.0941	0.0329, 0.0876	0.0231, 0.0529	0.0675, 0.175	0.0664, 0.1609

148.96 (Q), 151.47 (Q), 157.46 (Py); [Py = pyridine framework, Q = 5-chloro-8-hydroxyquinoline framework]. UV−vis: (MeCN, 25 °C) λ_{max} (ϵ_{max}) 250 (45 300), 332 nm (3800 dm^3 mol^{-1} cm^{-1}); (MeCN/H_2O 1:1 v/v, 25 °C): λ_{max} (ϵ_{max}) 250 (37 000), 332 nm (3100 dm^3 mol^{-1} cm^{-1}). MS (ES+): m/z 432 ([$\mathbf{L}^6$]$^+$).

Synthesis of $[Cu\mathbf{L}^5](ClO_4)_2 \cdot {}^1/_2MeCN$. $Cu(ClO_4)_2 \cdot 2H_2O$ (9.6 mg, 0.026 mmol) in MeCN (3 mL) was added to a solution of $\mathbf{L}^5$ (10.0 mg, 0.026 mmol) in MeCN (10 mL). The solution was stirred at room temperature under N_2 for 3 h. Green crystals were obtained by diffusion of Et_2O vapor into the reaction mixture (8.0 mg, 47%). Anal. Found (calcd) for $C_{22}H_{24.5}Cl_2CuN_{3.5}O_8S_2$: C, 39.80 (39.76); H, 3.70 (3.72); N, 7.35 (7.38); S, 9.60 (9.65%). MS (ES+): m/z 543 ([$Cu\mathbf{L}^5(ClO_4)$]$^+$).

Synthesis of $[Zn\mathbf{L}^5(H_2O)](ClO_4)_2$. $Zn(ClO_4)_2 \cdot 6H_2O$ (9.8 mg, 0.026 mmol) in MeCN (3 mL) was added to a solution of $\mathbf{L}^5$ (10.0 mg, 0.026 mmol) in MeCN (10 mL). The solution was stirred at room temperature under N_2 for 3 h. Colorless crystals were obtained by diffusion of Et_2O vapor into the reaction mixture (9.0 mg, 54%). Anal. Found (calcd) for $C_{21}H_{25}Cl_2N_3O_9S_2Zn$: C, 37.95 (38.00); H, 3.75 (3.80); N, 6.30 (6.33); S, 9.60 (9.66%). MS (ES+): m/z 546 ([$Zn\mathbf{L}^5(ClO_4)$]$^+$).

Synthesis of $[Hg\mathbf{L}^5(MeCN)](ClO_4)_2$. $Hg(ClO_4)_2 \cdot 3H_2O$ (12.0 mg, 0.026 mmol) in MeCN (3 mL) was added to a solution of $\mathbf{L}^1$ (10.0 mg, 0.026 mmol) in MeCN (10 mL). The solution was stirred at room temperature under N_2 for 3 h. Colorless crystals were obtained by diffusion of Et_2O vapor into the reaction mixture (10.0 mg, 48%). Anal. Found (calcd) for $C_{23}H_{26}Cl_2HgN_4O_8S_2$: C, 33.58 (33.60); H, 3.15 (3.19); N, 6.78 (6.82); S, 7.75 (7.80%). MS (ES+): m/z 682 ([$Hg\mathbf{L}^5(ClO_4)$]$^+$).

Synthesis of $[Pb\mathbf{L}^5(ClO_4)_2]$. $Pb(ClO_4)_2 \cdot 3H_2O$ (29.0 mg, 0.026 mmol) in MeCN (3 mL) was added to a solution of $\mathbf{L}^5$ (10.0 mg, 0.026 mmol) in MeCN (10 mL). The solution was stirred at room temperature under N_2 for 3 h. Colorless crystals were obtained by diffusion of Et_2O vapor into the reaction mixture (9.0 mg, 45%). Anal. Found (calcd) for $C_{21}H_{23}Cl_2N_3O_8PbS_2$: C, 32.00 (32.02); H, 2.90 (2.94); N, 5.35 (5.34); S, 8.10 (8.14%). MS (ES+): m/z 688 ([$Pb\mathbf{L}^5(ClO_4)$]$^+$).

Synthesis of $[Cu_3(5\text{-Cl-8-HDQH}_{-1})(\mathbf{L}^6H_{-1})_2](ClO_4)_3 \cdot 7.5H_2O$. $Cu(ClO_4)_2 \cdot 2H_2O$ (8.0 mg, 0.026 mmol) in MeCN (3 mL) was added to a solution of $\mathbf{L}^6$ (11.0 mg, 0.026 mmol) in MeCN (5 mL). The solution was allowed to stand, and after about 4 months, dark block crystals were formed (3.5 mg, 24%). Anal. Found (calcd) for $C_{51}H_{62}Cl_6Cu_3N_7O_{22.5}S_4$: C, 36.75 (36.80); H, 3.70 (3.75); N, 5.86 (5.89); S, 7.68 (7.70%). MS (ES+): m/z 1250 ([Cu_3(5-Cl-8-HDQH$_{-1}$)-($\mathbf{L}^6H_{-1})_2(H_3O)$]$^+$).

Synthesis of $[Cu(\mathbf{L}^6)_2](BF_4)_2 \cdot 2MeNO_2$. $Cu(BF_4)_2 \cdot H_2O$ (9.0 mg, 0.017 mmol) in $MeNO_2$ (3 mL) was added to a solution of $\mathbf{L}^6$ (15.0 mg, 0.035 mmol) in $MeNO_2$ (10 mL). The solution was stirred at room temperature under N_2 for 3 h. Green crystals were obtained by diffusion of Et_2O vapor into the reaction mixture (9.0 mg, 43%). Anal. Found (calcd) for $C_{44}H_{50}B_2Cl_2CuF_8N_8O_6S_4$: C, 43.18 (43.20); H, 4.10 (4.12); N, 9.14 (9.16); S, 10.58 (10.48%). MS (ES+): m/z 464 ([$Cu(\mathbf{L}^6)_2$]$^{2+}$).

Potentiometric Measurements. All pH measurements (pH = −log [H$^+$]) employed for the determination of ligand protonation and metal complex stability constants were carried out in a 0.10 M NMe_4Cl MeCN/H_2O (1:1, v/v) solution thermostated at 25 ± 0.1 °C using conventional titration experiments under an inert atmosphere. The choice of this solvent mixture was dictated by the low solubility of the ligands in pure water. The combined Ingold 405 S7/120 electrode was calibrated as a hydrogen concentration probe by titration of known amounts of HCl with CO_2-free NMe_4-OH solutions and determination of the equivalent point by Gran's method which allows one to determine the standard potential $E°$ and the ionic product of water (pK_w = 14.99(1) at 25 ± 0.1 °C in 0.1 mol dm^{-3} NMe_4Cl).[28] At least three measurements (with about 100 data points each) were performed for each system. In all experiments, the ligand concentration was about 1×10^{-3} mol dm^{-3}. In the complexation experiments, the metal ion concentration was varied from 0.3:1 to 0.9:1. The computer program HYPERQUAD[29] was used to calculate the equilibrium constants from the emf data. In the case of Hg^{II}, the potentiometric measurements were performed in 0.1 M NMe_4NO_3 ionic medium to avoid chloride competition in metal binding.

Crystallography. Crystal data and the refinement details for all structure determinations appear in Table 1. Only special features

(28) Gran, G. *Analyst* **1952**, *77*, 661.
(29) Gans, P.; Sabatini, A.; Vacca, A. *Talanta* **1996**, *43*, 1739.
(30) *SADABS, Area-Detector Absorption Correction Program*; Bruker AXS, Inc.: Madison, WI, 2003.
(31) *SHELXTL*, version 6.12; Bruker AXS Inc.: Madison, WI, 2001.
(32) (a) Blessing, R. H. *Acta Crystallogr., Sect. A* **1995**, *51*, 33. (b) Blessing, R. H. *J. Appl. Crystallogr.* **1997**, *30*, 421.

of the analyses are pointed out here. Single-crystal data collection for $[Cu\mathbf{L^5}](ClO_4)_2 \cdot {}^1/_2MeCN$, $[Zn\mathbf{L^5}(H_2O)](ClO_4)_2$, $[Pb\mathbf{L^5}(ClO_4)_2]$, and $[Cu_3(5\text{-Cl-8-HDQH}_{-1})(\mathbf{L^6}H_{-1})_2](ClO_4)_3 \cdot 7.5H_2O$ was performed on a Bruker SMART 1K CCD area detector diffractometer equipped with an Oxford Cryosystems open-flow cryostat,[33] using ω scans and graphite-monochromated Mo Kα radiation ($\lambda = 0.71073$ Å). The data collection for $[Hg\mathbf{L^5}(MeCN)](ClO_4)_2$ was carried out with a Bruker SMART APEX CCD area detector diffractometer using ω scans and graphite-monochromated Mo Kα radiation. Intensity data for $[Cu(\mathbf{L^6})_2](BF_4)_2 \cdot 2MeNO_2$ were collected, using φ and ω scans and Mo α radiation, monochromated by 10 cm confocal mirrors, on a Bruker-Nonius Kappa CCD diffractometer with a Bruker-Nonius FR591 rotating anode. All data sets were corrected for Lorentz, polarization, and absorption effects as specified in Table 1. With the exception of $[Cu\mathbf{L^5}](ClO_4)_2 \cdot {}^1/_2MeCN$ and $[Cu_3(5\text{-Cl-8-HDQH}_{-1})(\mathbf{L^6}H_{-1})_2](ClO_4)_3 \cdot 7.5H_2O$, where the structure was solved using SIR92,[34] all the structures were solved by direct methods using SHELXS97.[35] The structures were completed by iterative cycles of full-matrix least-squares refinement and ΔF syntheses using SHELXL97.[36] All non-H atoms, except for those in a disordered group, were refined anisotropically, and H atoms were introduced at calculated positions and refined using a riding model. In $[Cu\mathbf{L^5}](ClO_4)_2 \cdot {}^1/_2MeCN$, $[Zn\mathbf{L^5}(H_2O)](ClO_4)_2$, $[Hg\mathbf{L^5}(MeCN)](ClO_4)_2$, and $[Cu(\mathbf{L^6})_2](BF_4)_2 \cdot 2MeNO_2$, the H atoms on the solvent molecules were located from difference maps and refined as part of rigid groups and with restraints where necessary. In $[Cu_3(5\text{-Cl-8-HDQH}_{-1})(\mathbf{L^6}H_{-1})_2](ClO_4)_3 \cdot 7.5H_2O$, the perchlorate anion centered on Cl(4) was found to be disordered by rotation about the Cl(4)−O(10) vector: refinement showed that the two orientations both had half-occupancy for each of the three unique oxygen atoms. During the refinement, appropriate restraints were also applied to the Cl−O distances and O−Cl−O angles in the disordered perchlorate anion. In $[Cu_3(5\text{-Cl-8-HDQH}_{-1})(\mathbf{L^6}H_{-1})_2](ClO_4)_3 \cdot 7.5H_2O$, it was not possible to incorporate the solvent molecules in terms of discrete atomic sites; we therefore employed the SQUEEZE function in PLATON[37] to identify a diffuse electron density of 150 electrons per unit cell and a void volume of 410 Å^3. We assigned this electron density to 15 molecules of water per unit cell, in good agreement with the microanalytical data.

Results and Discussion

Optical Response of $\mathbf{L^5}$ in the Presence of Cu^{II}, Zn^{II}, Cd^{II}, Hg^{II}, and Pb^{II}. The optical response of $\mathbf{L^5}$ and $\mathbf{L^6}$ to Cu^{II}, Zn^{II}, Cd^{II}, Hg^{II}, and Pb^{II} was preliminarily investigated in the solvent mixture [MeCN/H_2O (4:1 v/v)] previously used for the same studies on $\mathbf{L^2}$−$\mathbf{L^4}$, which were scarcely soluble in other mixtures containing a higher content of water.[26] Subsequently, we noted that identical results were obtainable in MeCN/H_2O (1:1 v/v); therefore, we chose this last mixture of solvents for our studies on $\mathbf{L^5}$ and $\mathbf{L^6}$ because in it the binding properties of the two ligands could also easily be studied potentiometrically (see below). The absorption spectrum of a MeCN/H_2O (1:1 v/v, 25 °C) solution of $\mathbf{L^5}$ presents a large and unstructured band at 227 nm ($\epsilon = 39\,100$ dm^3 mol^{-1} cm^{-1}) and three other less intense ones at 273 (8000), 302 (3600), and 316 nm (4000 dm^3 mol^{-1} cm^{-1}). In the same mixture of solvents $\mathbf{L^5}$ exhibits an emission band at 382 nm with very low fluorescence quantum yield ($\Phi = 0.001$), when excited at 316 nm. The low fluorescence quantum yield can be attributed to a photoinduced electron transfer (PET) between the tertiary nitrogen atom of the macrocyclic moiety and the quinoline fragment.[1] Because the fluorescence of this type of molecular sensor is often pH sensitive,[38] we initially studied the effect of pH on the fluorescence of both $\mathbf{L^5}$ and its 1:1 metal complexes with Cu^{II}, Zn^{II}, Cd^{II}, Hg^{II}, or Pb^{II} in MeCN/H_2O (1:1 v/v, 25 °C). $\mathbf{L^5}$ does not change its fluorescence "OFF" state significantly over the range of pH considered (Figure 1a). A remarkable chelation enhancement of fluorescence (CHEF effect) is only observed in the presence of Zn^{II} (1 equiv) in the pH range of 3.0−9.0 with a maximum at around pH 7.0. The presence of the other metal ions does not significantly affect the OFF state of the sensor (Figure 1a). We therefore performed spectrofluorimetric titrations of $\mathbf{L^5}$ with Cu^{II}, Zn^{II}, Cd^{II}, Hg^{II}, or Pb^{II} in MeCN/H_2O (1:1 v/v, 25 °C) solutions buffered at pH 7.0 with HEPES. A significant CHEF effect ($I_{rel} = 800\%$) was observed only upon addition of Zn^{II} up to a $Zn^{II}/\mathbf{L^5}$ molar ratio of 1 (Figure 1b). The effect is not significant in the case of Cd^{II} ($I_{rel} = 70\%$). A Job plot analysis revealed that $\mathbf{L^5}$ binds 1 equiv of Zn^{II} (Figure 1c). Compared to *N*,*N*,*N*′,*N*′-tetrakis(2-quinolylmethyl)ethylenediamine (TQEN) whose optical response to metal ions was studied in DMF/H_2O (1:1 v/v),[39] the fluorescence switching "ON" effect observed for $\mathbf{L^5}$ in the presence of Zn^{II} is much larger (a 22-fold increase in the fluorescence emission intensity was observed for TQEN) and specific (the emission intensity of the complex TQEN-Cd^{II} is about 60% of that measured for the TQEN-Zn^{II} complex, whereas that of the complex $\mathbf{L^5}$-Cd^{II} is only 9% of that recorded for the complex $\mathbf{L^5}$-Zn^{II}).[39]

Significant changes were also observed in the UV−vis spectrum of the ligand upon addition of Zn^{II} or Cd^{II} to MeCN/H_2O (1:1 v/v, 25 °C) solutions of $\mathbf{L^5}$ buffered at pH 7.0. In particular, the band at 227 nm disappears, and a new one develops at around 240 nm (see Figure 1d for Zn^{II}). Furthermore, the band at 273 nm decreases, and those at 302 and 316 nm increase; the presence of well-defined isosbestic points suggests the presence of only two species in equilibrium. Similar changes were observed in the UV−vis spectrum of $\mathbf{L^5}$ upon addition of Cu^{II}, Hg^{II}, or Pb^{II}.

Optical Response of $\mathbf{L^6}$ in the Presence of Cu^{II}, Zn^{II}, Cd^{II}, Hg^{II}, and Pb^{II}. The absorption spectrum of a solution of $\mathbf{L^6}$ in MeCN/H_2O (1:1 v/v) presents a sharp band at 250 nm ($\epsilon = 37\,000$ dm^3 mol^{-1} cm^{-1}) and a broad one at 332 nm (3100 dm^3 mol^{-1} cm^{-1}). The latter corresponds to a weak emission band at 520 nm with a very low fluorescence quantum yield ($\Phi = 0.0001$). According to the literature, low values of fluorescence quantum yield in similar ligands have been attributed to two different mechanisms, namely, an intramolecular photoinduced proton transfer (PPT) between the hydroxyl group and the quinoline nitrogen and a

(33) Cosier, J.; Glazer, A. M. *J. Appl. Crystallogr.* **1986**, *19*, 105.
(34) Altomare, A.; Burla, M. C.; Camalli, M.; Cascarano, G.; Giacovazzo, C.; Gagliardi, A.; Polidori, G. *J. Appl. Crystallogr.* **1994**, *27*, 435.
(35) Sheldrick, G. M. *Acta Crystallogr., Sect. A* **1990**, *46*, 467.
(36) Sheldrick, G. M. *SHELXL97-2*; University of Göttingen: Göttingen Germany, 1998.
(37) Spek, A. L. *J. Appl. Crystallogr.* **2003**, *36*, 7−13.
(38) de Silva, S. A.; Zavaleta, A.; Baron, D. E.; Allam, O.; Isidor, E. V.; Kashimura, N.; Percarpio, J. M. *Tetrahedron Lett.* **1997**, *38*, 2237.
(39) Mikata, Y.; Wakamatsu, M.; Yano, S. *Dalton Trans.* **2005**, 545.

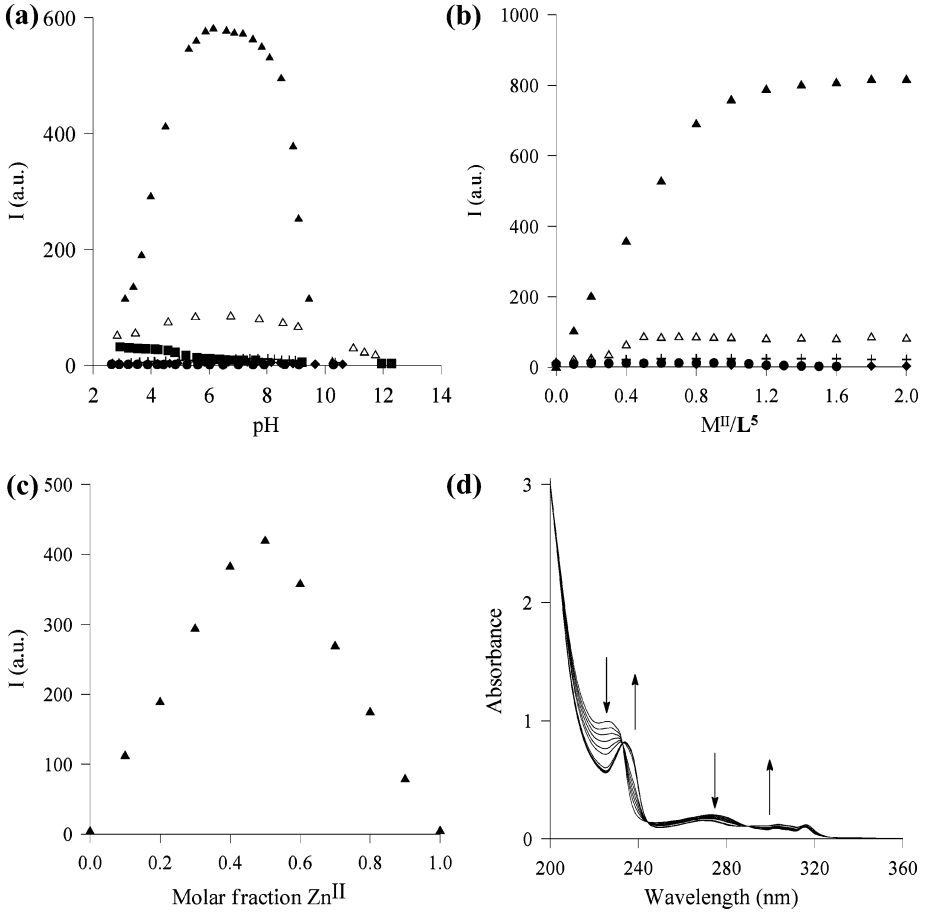

Figure 1. (a) Effect of pH on the fluorescence intensity at 382 nm of $\mathbf{L^5}$ (2.5×10^{-5} M, MeCN/H_2O (1:1 v/v), 25 °C) in the absence (■) and presence of Cu^{II} (●), Zn^{II} (▲), Cd^{II} (△), Hg^{II} (◆), and Pb^{II} (+) ($\lambda_{ex} = 316$ nm). (b) Fluorescent intensity/molar ratio plots for $\mathbf{L^5}$ (2.5×10^{-5} M, MeCN/H_2O (1:1 v/v), pH = 7.0, 25 °C) in the presence of increasing amounts of Cu^{II} (●), Zn^{II} (▲), Cd^{II} (Δ), Hg^{II} (◆); the addition of a Pb^{II}(+) amount higher than 0.6 equiv appeared to cause precipitation. (c) Job's plot for fluorescence intensity of the $\mathbf{L^5}$-Zn^{II} complex in MeCN/H_2O (1:1 v/v) at 25 °C, pH = 7.0; the sum of concentration of $\mathbf{L^5}$ and Zn^{II} is $4.72\ 10^{-5}$ M. (d) Changes in the absorption spectrum of $\mathbf{L^5}$ upon addition of increasing amounts of Zn^{II}. Isosbestic points occur at 232, 244, and 290 nm.

PET between the nitrogen atom of the macrocycle and the quinoline derivative.[40] In addition, in protic media, intermolecular PPT processes involving solvent molecules can also occur, further decreasing the fluorescence quantum yield of this kind of fluorophore.[40] Figure 2a clearly shows that $\mathbf{L^6}$ in MeCN/H_2O (1:1 v/v, 25 °C) maintains the OFF state in the pH range explored and that the presence of Cu^{II}, Zn^{II}, Hg^{II}, or Pb^{II} (1 equiv) does not turn ON the fluorescence of the ligand on changing the pH. A significant CHEF effect is only observed in the presence of Cd^{II} (1 equiv) in the pH range of 4.0−9.0 with a maximum at around pH 6.0. Spectrofluorimetric titrations of $\mathbf{L^6}$ with Cu^{II}, Zn^{II}, Cd^{II}, Hg^{II}, or Pb^{II} in MeCN/H_2O (1:1 v/v, 25 °C) solutions buffered at pH 7.0 with HEPES confirmed this significant CHEF effect recorded upon addition of Cd^{II} ($I_{rel} = 180\%$, after the addition of 2 equiv of metal ion; Figure 2b), and the inflection point in the fluorescence intensity/molar ratio plot (Figure 2b) suggested the formation of the 1:1 $[Cd\mathbf{L^6}]^{2+}$ complex cation during the spectrofluorimetric titration, as also supported by a Job's plot (Figure 2c). According to the literature, this remarkable increase in the fluorescence intensity can be attributed to the fact that both the PPT and PET processes are inhibited in the fluorescent 1:1 Cd^{II} complex with $\mathbf{L^6}$.[40] The titration curve of $\mathbf{L^6}$ with Zn^{II} in the same experimental conditions as with Cd^{II} shows a much less prominent CHEF effect with inflection points at $Zn^{II}/\mathbf{L^6}$ values of 0.5 and 1, which seems to indicate the formation in solution of the species $[Zn(\mathbf{L^6})_2]^{2+}$ and $[Zn\mathbf{L^6}]^{2+}$ (Figure 2b). The effects of metal ion complexation on the absorption properties of $\mathbf{L^6}$ in MeCN/H_2O (1:1 v/v, 25 °C) solutions buffered at pH 7.0 were in general significant and similar for all metal ions considered: the bands at 250 and 332 nm disappear, and new ones develop isosbestically at about 260 and 360 nm (Figure 2d for Cd^{II}). In the case of Zn^{II}, the isosbestic points were not maintained upon addition of excess metal ion beyond the $Zn^{II}/\mathbf{L^6}$ molar ratio of 0.5.

We also performed spectrofluorimetric titrations of $\mathbf{L^6}$ with Cu^{II}, Zn^{II}, Cd^{II}, Hg^{II}, or Pb^{II} in MeCN (25 °C). Interestingly, in these experimental conditions, $\mathbf{L^6}$ is in an ON state, and the formation of 1:2 $[M(\mathbf{L^6})_2]^{2+}$ species during titrations seems to be the rule (Figure 3). In fact, a complete chelation-induced quenching of fluorescence was observed upon addition of Cu^{II}, Hg^{II}, or Pb^{II} up to a $M^{II}/\mathbf{L^6}$ molar ratio of 0.5 (Figure 3), whereas the addition of Cd^{II} or Zn^{II} resulted in a quenching effect observed up to a molar ratio of 0.5,

(40) Farruggia, G.; Iotti, S.; Prodi, L.; Montalti, M.; Zaccheroni, N.; Savage, P. B.; Trapani, V.; Sale, P.; Wolf, F. I. *J. Am. Chem. Soc.* **2006**, *128*, 344 and references therein.

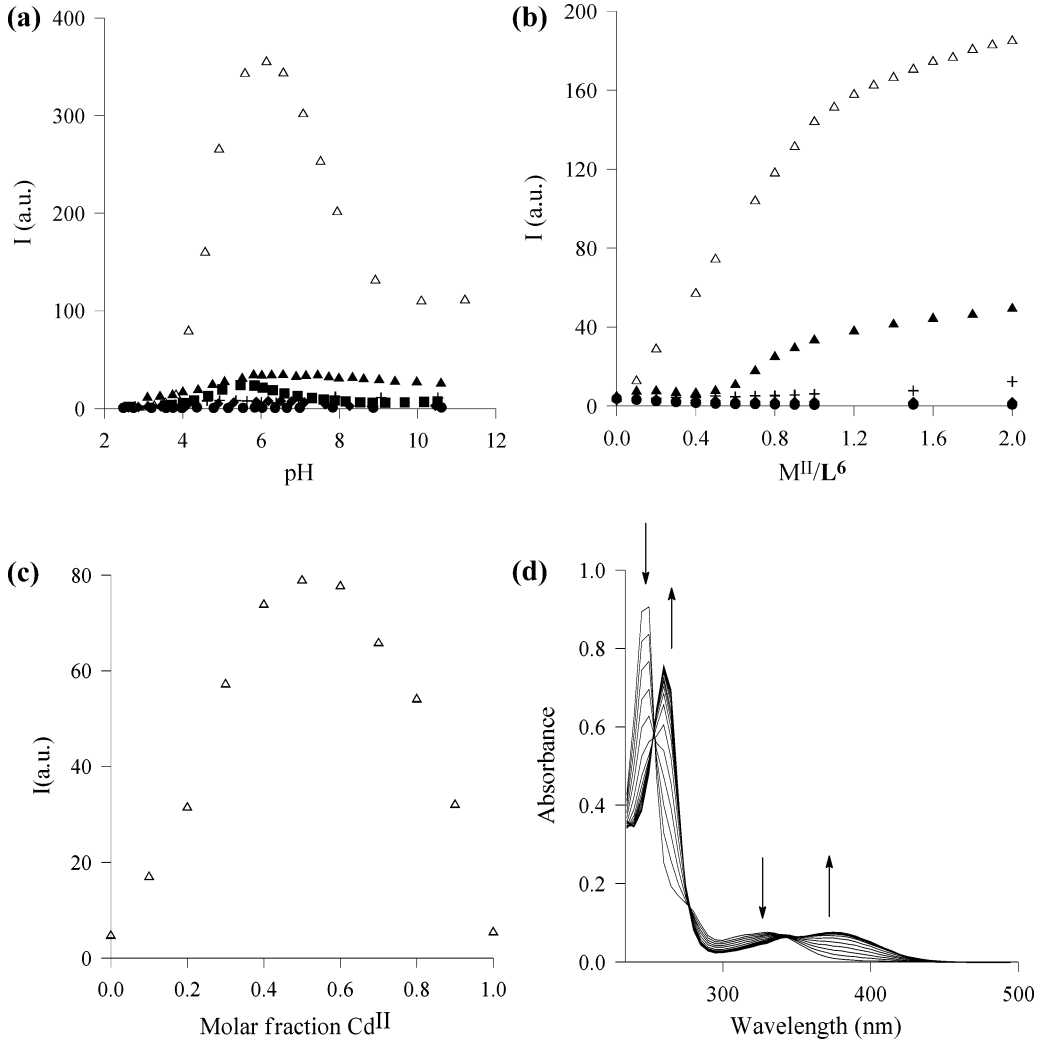

Figure 2. (a) Effect of pH on fluorescence intensity at 520 nm of $\mathbf{L^6}$ (2.5×10^{-5} M, MeCN/H_2O (1:1 v/v), 25 °C) in the absence (■) and presence of Cu^{II} (●), Zn^{II} (▲), Cd^{II} (△), Hg^{II} (◆), and Pb^{II} (+) ($\lambda_{ex} = 332$ nm). (b) Fluorescent intensity/molar ratio plots for $\mathbf{L^6}$ (2.5×10^{-5} M, MeCN/H_2O (1:1 v/v), pH = 7.0, 25 °C) in the presence of increasing amounts of Cu^{II} (●), Zn^{II} (▲), Cd^{II} (△), Hg^{II} (◆), and Pb^{II}(+). (c) Job's plot for fluorescence intensity of $\mathbf{L^6}$-Cd^{II} complex in MeCN/H_2O (1:1 v/v) at 25 °C, pH = 7.0; the sum of concentration of $\mathbf{L^6}$ and Cd^{II} is 5.38 10^{-5} M. (d) Changes in the absorption spectrum of $\mathbf{L^6}$ upon addition of increasing amounts of Cd^{II}. Isosbestic points occur at 253, 277, and 344 nm.

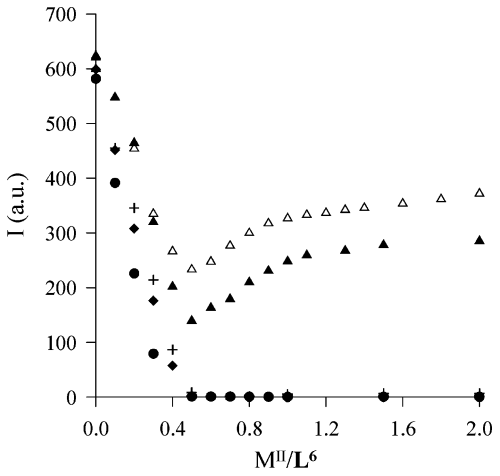

Figure 3. Fluorescent intensity/molar ratio plots for $\mathbf{L^6}$ (2.5×10^{-5} M, MeCN, 25 °C) in the presence of increasing amounts of Cu^{II} (●), Zn^{II} (▲), Cd^{II} (△), Hg^{II} (◆), and Pb^{II}(+).

followed by a CHEF effect until a $M^{II}/\mathbf{L^6}$ molar ratio of 1 was reached (Figure 3). Analogous measurements performed for $\mathbf{L^5}$ showed a CHEF effect only for Zn^{II} and a less pronounced one for Cd^{II}, as observed in MeCN/H_2O (1:1 v/v, 25 °C) (see above), with inflection points in the titration curves corresponding to the formation of 1:1 $[M\mathbf{L^6}]^{2+}$species ($M^{II} = Zn^{II}$, Cd^{II}).

Coordination Properties in Solution of $\mathbf{L^5}$ and $\mathbf{L^6}$ Toward Cu^{II}, Zn^{II}, Cd^{II}, Hg^{II}, and Pb^{II}. To gain a deeper insight into the nature of the complex species formed during the spectrofluorimetric titrations of $\mathbf{L^5}$ and $\mathbf{L^6}$ with Cu^{II}, Zn^{II}, Cd^{II}, Hg^{II} and Pb^{II}, we investigated protonation and complex formation of the two ligands by means of potentiometric measurements in MeCN/H_2O (1:1 v/v) mixtures at 25 °C. Both ligands can bind up to two protons in MeCN/H_2O (1:1 v/v). The value of the first basicity constant (calculated log *K* values are 6.65(7) and 7.6(1) for $\mathbf{L^5}$ and $\mathbf{L^6}$, respectively) accounts for the protonation of the aliphatic tertiary amine group of the macrocyclic framework.[41] A second protonation step takes place at more acidic pH values (calculated log *K* values are 1.8(1) and 3.2(1) for $\mathbf{L^5}$ and $\mathbf{L^6}$, respectively),

(41) Bencini, A.; Bianchi, A.; Garcia-España, E.; Micheloni, M.; Ramirez, J. A. *Coord. Chem. Rev.* **1999**, *188*, 97.

Table 2. Formation Constants (log *K*) of the Metal Complexes with $\mathbf{L^5}$ and $\mathbf{L^6}$ ($I = 0.1$ M, 25 °C)

reaction	log *K*				
	Cu^{II}[a]	Zn^{II}[a]	Cd^{II}[a]	Pb^{II}[a]	Hg^{II}[b]
$M^{II} + \mathbf{L^5} \rightleftharpoons [M\mathbf{L^5}]^{2+}$	8.9(1)	7.20(4)	7.92(6)	*c*	9.1(1)
$[M\mathbf{L^5}]^{2+} + OH^- \rightleftharpoons [M\mathbf{L^5}(OH)]^+$					5.7(1)
$M^{II} + \mathbf{L^6} \rightleftharpoons [M\mathbf{L^6}]^{2+}$	9.53(3)	7.9(1)	9.33(5)	9.06(7)	9.5(1)
$M^{II} + 2\mathbf{L^6} \rightleftharpoons [M(\mathbf{L^6})_2]^{2+}$		14.6(1)			
$M^{II} + 2\mathbf{L^6} + 2H_2O \rightleftharpoons [M(\mathbf{L^6}H_{-1})_2] + 2H_3O^+$		−4.5(1)			

[a] Measurements were carried out in 0.1 M NMe_4Cl. [b] Measurements were carried out in 0.1 M NMe_4NO_3. [c] The low solubility of the Pb^{II} complexes with $\mathbf{L^5}$ did not allow the potentiometric study of this system.

and it should involve a weakly basic nitrogen atom belonging to an heteroaromatic moiety. In fact, the nitrogen atoms of the pyridine, quinoline, and 5-chloro-8-hydroxy-quinoline frameworks are characterized by similar basicity properties, and therefore, the potentiometric measurements do not allow differentiation of the second protonation site.[42] Furthermore, it is known that 5-chloro-8-hydroxy-quinoline can be also deprotonated at strongly alkaline pH ($pK_a = 10.64$ in water/dioxane 60:40 v/v mixtures),[43] but under our experimental conditions (pH range = 2.5−10.5), no deprotonation of the hydroxyl group was monitored for $\mathbf{L^6}$.

The potentiometric study of metal complexation of the two ligands in MeCN/H_2O (1:1 v/v, 25 °C) was generally limited to the acidic pH region because of complex precipitation beyond neutral pH values. Only for the two systems $Hg^{II}/\mathbf{L^5}$ and $Zn^{II}/\mathbf{L^6}$, the potentiometric measurements were carried out over a wider pH range (including the alkaline region up to pH 10.0). All metals form stable 1:1 complexes at acidic pH values with both $\mathbf{L^5}$ and $\mathbf{L^6}$. In the case of Zn^{II} with $\mathbf{L^6}$, the formation of complexes with a 1:2 metal-to-ligand stoichiometry is also observed. The species formed and the corresponding stability constants are reported in Table 2. However, for the system $Pb^{II}/\mathbf{L^5}$, scarcely soluble complexes formed at even acidic pH values, preventing any analysis of this system. For both ligands, the stability of the 1:1 complexes increases in the order $Zn^{II} < Pb^{II} < Cd^{II} < Cu^{II} \leq Hg^{II}$ (although the value of log *K* for the complexation of Pb^{II} by $\mathbf{L^5}$ could not be measured), as previously observed for the unfunctionalized macrocycle 2,8-dithia-5-aza-2,6-pyridinophane ($\mathbf{L^1}$).[26] The 1:1 complexes with Cu^{II} and Hg^{II} display higher stability, a feature common to complexes with polyamine ligands. In contrast, the lower stability of the Zn^{II} complexes with respect to the Cd^{II} and Pb^{II} ones might seem somewhat surprising, since polyamine ligands often show a similar binding ability toward these three metal ions. On the other hand, $\mathbf{L^5}$ and $\mathbf{L^6}$ contain within their macrocyclic framework two soft sulfur donors, which generally display a higher binding ability toward the softer Cd^{II} and Pb^{II} ions. Table 2 clearly shows that $\mathbf{L^6}$ forms slightly more stable 1:1 complexes than $\mathbf{L^5}$ with all metal ions considered. It is reasonable to suppose that in all 1:1 complexes with both ligands the coordinating groups belonging to the fluorogenic fragment are involved in metal coordination, in particular, the deprotonated hydroxyl function of the 5-chloro-8-hydroxy-quinoline unit in $\mathbf{L^6}$, thereby leading to the observed order of complex stabilities. In fact, while quinoline generally does not show a marked tendency to bind metal cations, 5-chloro-8-hydroxy-quinoline (5-Cl-8-HDQ) shows a marked tendency to deprotonate upon metal binding, thus affording remarkably stable 1:1 and 1:2 complexes with transition metal ions such as Cu^{II} or Zn^{II}.[42,44] The stability of the 1:1 Cu^{II} and Zn^{II} complexes with deprotonated 5-Cl-8-HDQ is comparable to or higher than that calculated for the analogous 1:1 complexes with $\mathbf{L^6}$: for example, in water/dioxane (6:4 v/v) mixtures, log $K = 9.0$ and 17.85 for the equilibria $Zn^{II} + (\text{5-Cl-8-HDQH}_{-1})^- \rightleftharpoons [Zn(\text{5-Cl-8-HDQH}_{-1})]^+$ and $[Zn(\text{5-Cl-8-HDQH}_{-1})]^+ + (\text{5-Cl-8-HDQH}_{-1})^- \rightleftharpoons [Zn(\text{5-Cl-8-HDQH}_{-1})_2]$, respectively.[44] Although potentiometric measurements do not give information on the structure of the complex species formed, the high tendency of 5-Cl-8-HDQ in its deprotonated form to bind metal ions suggests that in the 1:1 complexes $[M\mathbf{L^6}]^{2+}$ (M = Cu^{II}, Zn^{II}, Cd^{II}, Hg^{II}, and Pb^{II}) the metal ions might be coordinated to the deprotonated 5-Cl-8-HDQ unit of $\mathbf{L^6}$, an acidic proton being localized on either the amine group of the macrocycle moiety or the nitrogen donor of the quinoline framework. This structural hypothesis would also agree with the UV−vis and spectrofluorimetric measurements (see above).

Interestingly, for the $Zn^{II}/\mathbf{L^6}$ system, which was potentiometrically investigated over a wider pH range (2.0−10.0), the almost concomitant formation of the 1:1 $[Zn\mathbf{L^6}]^{2+}$ and 1:2 $[Zn(\mathbf{L^6})_2]^{2+}$complexes is observed at acidic pH values (Table 2, Figure 4), in good agreement with the spectrofluorimetric measurements (see above and Figure 2b). Deprotonation of the $[Zn(\mathbf{L^6})_2]^{2+}$ complex at alkaline pH values affords the 1:2 neutral complex $[Zn(\mathbf{L^6}H_{-1})_2]$ (Table 2 and Figure 4). Of course these data do not give any information on the possible isomers present in solution for 1:2 metal-to-ligand complexes with $\mathbf{L^6}$.

Presumably, 1:2 complex species with Cu^{II}, Cd^{II}, Hg^{II}, and Pb^{II} are also formed at higher pH values in MeCN/H_2O (1:1 v/v) mixtures but are too insoluble to be detected potentiometrically. These complex species appear, however, to form preferentially in MeCN solutions (Figure 3).

The comparison between the distribution curves derived from the potentiometric measurements and the pH dependence of the fluorescence emission at 382 nm for the $Zn^{II}/\mathbf{L^5}$ system (Figure 4b) clearly indicates that the species $[Zn(\mathbf{L^5})]^{2+}$ is responsible for the CHEF effect observed at

(42) Smith, R. M.; Martell, A. *NIST Stability Constants Database*, version 4.0; National Institute of Standards and Technology: Washington, DC, 1997.
(43) Steger, H.; Corsini, A.; *J. Inorg. Nucl. Chem*. **1973**, *35*, 1621.
(44) Geshon, H.; McNeil, M.; Schulman, S. *Anal. Chim. Acta* **1972**, *62*, 43.

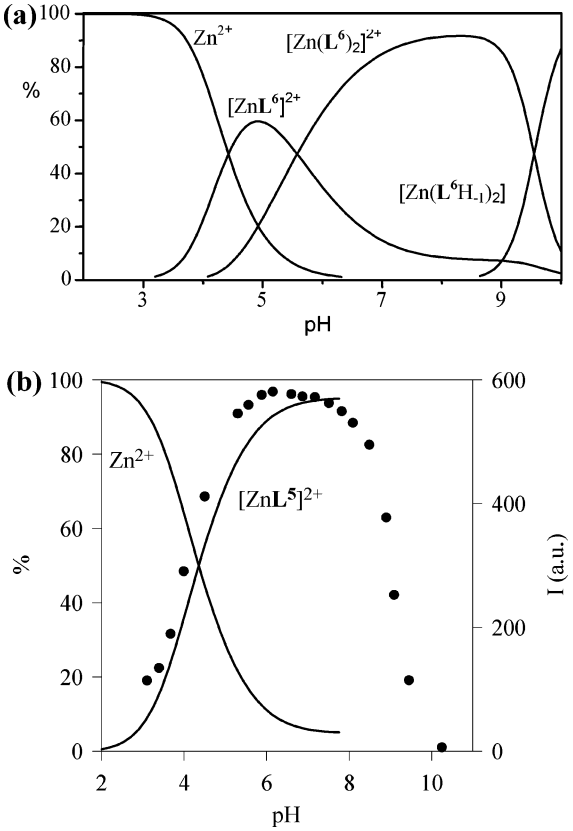

Figure 4. (a) Distribution diagram for the system $Zn^{II}/\mathbf{L^6}$ in MeCN/H_2O (1:1 v/v) (I = 0.1 M, 25 °C, [$\mathbf{L^6}$] = 5×10^{-5} M, [Zn^{II}] = 2.5×10^{-5} M). (b) Distribution diagram for the system $Zn^{II}/\mathbf{L^5}$ in MeCN/H_2O (1:1 v/v) (I = 0.1 M, 25 °C, [$\mathbf{L^5}$] = [Zn^{2+}] = 2.5×10^{-5} M) and (●) spectrofluorimetric data from Figure 1a.

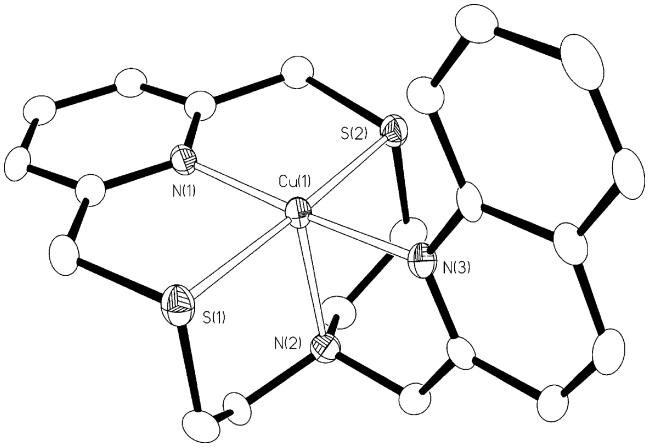

Figure 5. Ellipsoid plot showing one of the two independent $[Cu\mathbf{L^5}]^{2+}$ complex cations in $[Cu\mathbf{L^5}](ClO_4)_2 \cdot {}^1/_2MeCN$ with the adopted numbering scheme. Displacement ellipsoids are drawn at 50% probability. Hydrogen atoms, ClO_4^- counteranions, and co-crystallized solvent molecules have been omitted for clarity.

acidic pH values upon addition of Zn^{II} to MeCN/H_2O (1:1 v/v) solutions of $\mathbf{L^5}$ (Figure 1). An analogous comparison for the $Cd^{II}/\mathbf{L^6}$ system allows us to explain the CHEF effect also observed in this case at acidic pH values upon addition of Cd^{II} to MeCN/H_2O (1:1 v/v) solutions of $\mathbf{L^6}$ (Figure 2) as being caused by the formation of the $[Cd(\mathbf{L^6})]^{2+}$ complex in solution.

In both cases, the subsequent return of the ligands to an OFF state at higher pH values (>7) could be the result of

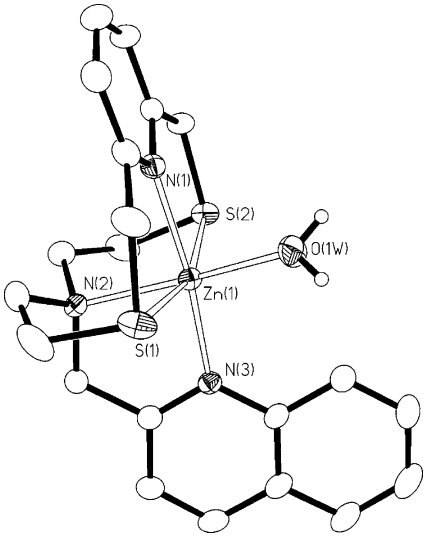

Figure 6. Ellipsoid plot of the complex cation $[Zn\mathbf{L^5}(H_2O)]^{2+}$ in $[Zn\mathbf{L^5}(H_2O)](ClO_4)_2$ with the adopted numbering scheme. Displacement ellipsoids are drawn at 50% probability. Hydrogen atoms, except those on the coordinated water molecule, and ClO_4^- counteranions have been omitted for clarity.

the formation of hydroxylated or 1:2 complex species in which either PPT, PET, or both are possibly restored. Unfortunately, it was not possible to confirm this potentiometrically because of the limited pH range investigable for both systems $Zn^{II}/\mathbf{L^5}$ and $Cd^{II}/\mathbf{L^6}$.

X-ray Crystallography. From the complexation reaction of $\mathbf{L^5}$ with the appropriate metal salt in MeCN, followed by diffusion of Et_2O vapor into the reaction mixture, we were able to grow single crystals of the complexes $[Cu\mathbf{L^5}](ClO_4)_2 \cdot {}^1/_2MeCN$, $[Zn\mathbf{L^5}(H_2O)](ClO_4)_2$, $[Hg\mathbf{L^5}(MeCN)](ClO_4)_2$, and $[Pb\mathbf{L^5}(ClO_4)_2]$ suitable for X-ray diffraction analysis. In all four complexes, $\mathbf{L^5}$ interacts with each metal center through all its donor atoms (Table 3 and Figures 5−8). As already observed in $[Cu\mathbf{L^1}(NO_3)_2]$, $[Zn\mathbf{L^1}(NO_3)_2]$ and $[Zn\mathbf{L^4}](NO_3)_2 \cdot MeNO_2$,[26] the macrocyclic framework of $\mathbf{L^5}$ adopts a folded conformation resembling an open book with the spine along the S(1)−M−S(2) direction and the N(1)−M−N(2) hinge angle increasing from 83.38(8) to 102.00(14)° in the order $Pb^{II} < Zn^{II} < Hg^{II} < Cu^{II}$ (Table 3). The aliphatic nitrogen is located almost perpendicular to the pseudoplane defined by the metal ion, the pyridine ring, and the two thioether sulfur atoms. One of the two mutually cis positions of a formal pseudo-octahedral coordination sphere left free by the N_2S_2-donor set of the macrocyclic framework is occupied by the N-donor atom of the quinoline moiety; the other is either left unoccupied to give an overall distorted square-based pyramidal geometry in $[Cu\mathbf{L^5}]^{2+}$(Figure 5, the asymmetric unit features two similarly complexed ligand molecules) or is occupied by a solvent molecule to afford an overall distorted octahedral geometry in $[Zn\mathbf{L^5}(H_2O)]^+$ (Figure 6) and $[Hg\mathbf{L^5}(MeCN)]^{2+}$ (Figure 7). In the complex $[Pb\mathbf{L^5}(ClO_4)_2]$, 9-coordination is instead achieved at the metal center, which resides in a $N_3S_2O_4$ environment, bound by the five donors of $\mathbf{L^5}$ and by two bidentate perchlorato ligands (Table 3, Figure 8). The Pb−O distances involving the two ClO_4^- ligands are considerably longer than those usually expected for oxygen-donating counteranions interact-

Table 3. Selected Bond Distances (Å) and Angles (deg) for [Cu**L**^{5}](ClO$_4$)$_2$·$^1/_2$MeCN,[a] [Zn**L**^{5}(H$_2$O)](ClO$_4$)$_2$, [Hg**L**^{5}(MeCN)](ClO$_4$)$_2$, and [Pb**L**^{5}(ClO$_4$)$_2$][b]

	[Cu**L**^{5}](ClO$_4$)$_2$·$^1/_2$MeCN	[Zn**L**^{5}(H$_2$O)](ClO$_4$)$_2$	[Hg**L**^{5}(MeCN)](ClO$_4$)$_2$	[Pb**L**^{5}(ClO$_4$)$_2$][c]
M−N(1)	1.967(3) [1.972(3)]	2.158(2)	2.508(3)	2.740(3)
M−N(2)	2.174(4) [2.189(4)]	2.214(2)	2.473(3)	2.571(3)
M−N(3)	1.975(3) [1.972(3)]	2.146(2)	2.378(3)	2.648(3)
M−S(1)	2.3369(12) [2.3381(11)]	2.4890(7)	2.6800(8)	2.8987(9)
M−S(2)	2.3369(11) [2.3445(11)]	2.4829(7)	2.6574(9)	2.9014(9)
M−X(1)		2.095(2)	2.313(4)	2.973(3) [2.991(3)]
M−X(2)				2.899(3) [3.167(3)]
N(1)−M−N(2)	102.00(14) [100.28(15)]	90.81(8)	94.87(10)	83.38(8)
N(1)−M−N(3)	175.45(17) [177.37(17)]	169.58(8)	162.57(11)	139.22(8)
N(1)−M−S(1)	87.34(10) [87.40(10)]	83.81(6)	74.88(6)	67.66(6)
N(1)−M−S(2)	87.57(11) [86.94(10)]	81.55(6)	74.00(6)	68.49(6)
N(1)−M−X(1)		83.49(8)	90.46(12)	144.42(8) [131.43(8)]
N(1)−M−X(2)				72.96(8) [68.40(8)]
N(2)−M−N(3)	82.54(15) [82.35(15)]	80.42(8)	71.88(10)	63.33(8)
N(2)−M−S(1)	88.94(10) [88.56(10)]	83.11(6)	78.16(7)	73.80(6)
N(2)−M−S(2)	89.41(10) [88.80(10)]	87.55(6)	79.11(7)	72.79(6)
N(2)−M−X(1)		166.98(8)	162.75(14)	123.19(8) [81.16(8)]
N(2)−M−X(2)				150.13(8) [139.66(8)]
N(3)−M−S(1)	92.38(9) [92.48(10)]	100.57(6)	112.04(7)	80.29(6)
N(3)−M−S(2)	92.92(9) [93.35(10)]	92.38(6)	92.00(7)	117.95(6)
N(3)−M−X(1)		106.23(8)	105.52(12)	76.31(8) [68.66(8)]
N(3)−M−X(2)				126.90(8) [152.12(8)]
S(1)−M−S(2)	174.20(4) [173.22(4)]	162.50(3)	139.35(3)	126.88(3)
S(1)−M−X(1)		84.65(6)	87.47(10)	137.70(6) [146.55(5)]
S(1)−M−X(2)				80.38(6) [117.37(5)]
S(2)−M−X(1)		103.09(6)	118.14(11)	95.29(6) [62.97(5)]
S(2)−M−X(2)				113.24(5) [70.34(5)]
X(1)−M−X(2)				46.41(7) [45.19(7)][d]

[a] Two molecules are present in the asymmetric unit of [Cu**L**^{5}](ClO$_4$)$_2$·$^1/_2$MeCN. [b] X(1) = O(1W) in [Zn**L**^{5}(H$_2$O)](ClO$_4$)$_2$, N(1S) in [Hg**L**^{5}(MeCN)](ClO$_4$)$_2$, and Cl(1)O$_4$ in [Pb**L**^{5}(ClO$_4$)$_2$]; X(2) = Cl(2)O$_4$ in [Pb**L**^{5}(ClO$_4$)$_2$]. [c] Where two values are reported, the first refers to bond distances and angles involving O(4) or O(3) and the second to bond distances and angles involving O(7) or O(6). [d] X(1)−M−X(2) = O(3)−Pb(1)−O(4) [O(6)−Pb(1)−O(7)].

Table 4. Selected Bond Distances (Å) and Angles (deg) for [Cu$_3$(5-Cl-8-HDQH$_{-1}$)(**L**^{6}H$_{-1}$)$_2$](ClO$_4$)$_3$·7.5H$_2$O

	Cu(1)	Cu(3)		Cu(2)
Cu−N(1)	2.000(7)	1.978(8)	Cu−O(1A)	2.357(6)
Cu−N(2)	2.188(7)	2.195(8)	Cu−O(1B)	2.338(6)
Cu−O(1)	1.922(5)	1.909(6)	Cu−O(1C)	2.059(8)
Cu−S(1)	2.359(3)	2.366(3)	Cu−N(3A)	2.030(8)
Cu−S(2)	2.386(3)	2.347(3)	Cu−N(3B)	2.030(7)
			Cu−N(3C)	1.999(9)
N(1)−Cu−N(2)	98.3(3)	109.6(3)		
N(1)−Cu−O(1)	166.1(3)	156.2(3)	O(1A)−Cu−O(1B)	171.2(2)
N(1)−Cu−S(1)	87.6(2)	87.1(3)	O(1A)−Cu−O(1C)	89.0(3)
N(1)−Cu−S(2)	86.3(2)	86.6(3)	O(1A)−Cu−N(3A)	76.1(3)
N(2)−Cu−O(1)	95.6(2)	94.1(3)	O(1A)−Cu−N(3B)	97.7(3)
N(2)−Cu−S(1)	87.6(2)	85.9(2)	O(1A)−Cu−N(3C)	93.6(3)
N(2)−Cu−S(2)	87.3(2)	89.4(2)	O(1B)−Cu−O(1C)	98.0(3)
S(1)−Cu−O(1)	92.82(19)	96.62(19)	O(1B)−Cu−N(3A)	96.6(3)
S(1)−Cu−S(2)	171.44(10)	170.42(11)	O(1B)−Cu−N(3B)	77.1(3)
S(2)−Cu−O(1)	94.55(19)	92.05(19)	O(1B)−Cu−N(3C)	92.2(3)
			O(1C)−Cu−N(3A)	164.8(3)
			O(1C)−Cu−N(3B)	89.2(3)
			O(1C)−Cu−N(3C)	85.9(4)
			N(3A)−Cu−N(3B)	90.2(3)
			N(3A)−Cu−N(3C)	97.6(4)
			N(3B)−Cu−N(3C)	167.6(4)
Cu(1)−O(1A)−Cu(2)		116.0(3)		
Cu(2)−O(1B)−Cu(3)		111.8(3)		

ing with Pb^{II}.[22,45] This structural feature might indicate the presence in [Pb**L**^{5}(ClO$_4$)$_2$] of a stereochemically active 6s^2 lone pair positioned in the coordination hemisphere not occupied by the donor set of **L**^{5}. In all four complexes, the M−S bond lengths are longer than the metal bond distances involving the other donor atoms of **L**^{5}; furthermore, the S(1)−M−S(2) angle decreases from 174.20(4) to 126.88(3)° in the order Cu^{II} > Zn^{II} > Hg^{II} > Pb^{II}, and this corresponds to an increase in the M−N(1) distance from 1.967(3) (for [Cu**L**^{5}]$^{2+}$) to 2.740(3) Å (for [Pb**L**^{5}(ClO$_4$)$_2$]) and, therefore, to a gradual displacement of the metal ion from the ring cavity of the macrocyclic framework.

Unfortunately, we were unable to grow single crystals of 1:1 complexes between **L**^{6} and the metal ions under

(45) Blake, A. J.; Fenske, D.; Li, W.-S.; Lippolis, V.; Schröder, M. *J. Chem. Soc., Dalton Trans.* **1998**, 3961.

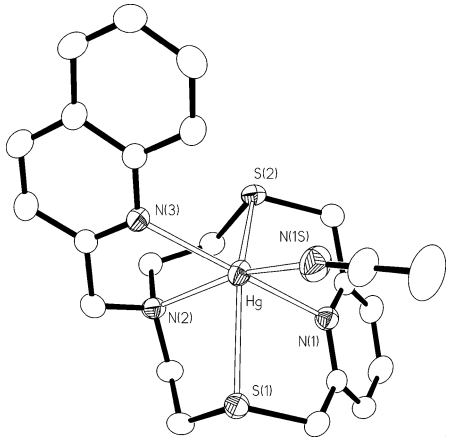

Figure 7. Ellipsoid plot showing the complex cation $[Hg\mathbf{L}^5(MeCN)]^{2+}$ in $[Hg\mathbf{L}^5(MeCN)](ClO_4)_2$ with the adopted numbering scheme. Displacement ellipsoids are drawn at 50% probability. Hydrogen atoms and ClO_4^- counteranions have been omitted for clarity.

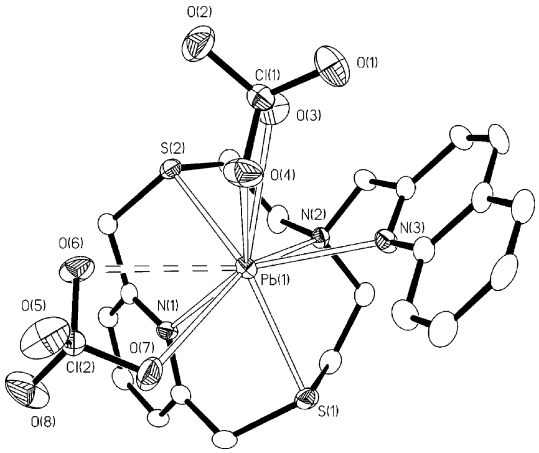

Figure 8. Ellipsoid plot showing $[Pb\mathbf{L}^5(ClO_4)_2]$ with the adopted numbering scheme. Displacement ellipsoids are drawn at 50% probability. Hydrogen atoms have been omitted for clarity.

investigation. However, after several months of standing at room temperature, a MeCN solution containing a 1:1 reaction molar ratio of $\mathbf{L}^6$ and $Cu(ClO_4)_2 \cdot 2H_2O$ fortuitously produced dark red crystals. Although the relatively poor quality of the X-ray diffraction from these crystals precluded a full analysis, we were able to establish the formation of $[Cu_3(5\text{-Cl-8-HDQH}_{-1})(\mathbf{L}^6\mathrm{H}_{-1})_2](ClO_4)_3 \cdot 7.5H_2O$ (Table 4, Figure 9) as a trinuclear Cu^{II} complex in which two $[Cu(\mathbf{L}^6\mathrm{H}_{-1})]^+$ units, each featuring a deprotonated $\mathbf{L}^6$ imposing a distorted square-based pyramidal coordination sphere at the metal center, interact through the donor atoms of the hydroxyquinoline moieties with a $[Cu(5\text{-Cl-8-HDQH}_{-1})]^+$ cation. The metal ion in the central position of the trinuclear system is, therefore, formally coordinated to three $(5\text{-Cl-8-HDQH}_{-1})^{-1}$ moieties in a pseudooctahedral coordination sphere: two of them belong to as many $[Cu(\mathbf{L}^6\mathrm{H}_{-1})]^+$ units, and the third derives from an $\mathbf{L}^6$ molecule via cleavage of the pendent arm. The three metal centers are bridged by the two deprotonated hydroxyl functions belonging to the two $[Cu(\mathbf{L}^6\mathrm{H}_{-1})]^+$ units. The remaining crystals of $[Cu_3(5\text{-Cl-8-HDQH}_{-1})(\mathbf{L}^6\mathrm{H}_{-1})_2](ClO_4)_3 \cdot 7.5H_2O$ were dissolved in MeCN

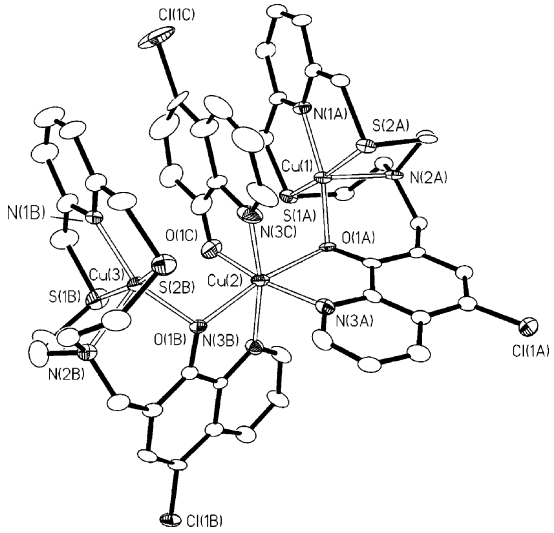

Figure 9. Ellipsoid plot of the trinuclear complex cation $[Cu_3(5\text{-Cl-8-HDQH}_{-1})(\mathbf{L}^6\mathrm{H}_{-1})_2]^{3+}$ in $[Cu_3(5\text{-Cl-8-HDQH}_{-1})(\mathbf{L}^6\mathrm{H}_{-1})_2](ClO_4)_3 \cdot 7.5H_2O$ with the adopted numbering scheme. Displacement ellipsoids are drawn at 30% probability. Hydrogen atoms and ClO_4^- counteranions have been omitted for clarity.

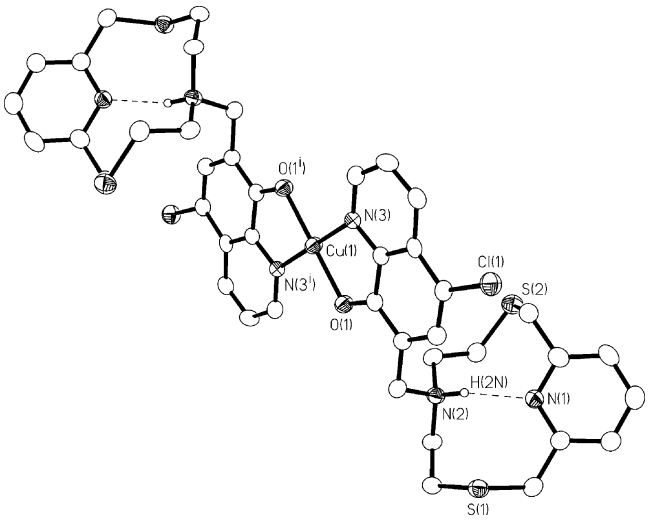

Figure 10. Ellipsoid plot showing the complex cation $[Cu(\mathbf{L}^6)_2]^{2+}$ in $[Cu(\mathbf{L}^6)_2](BF_4)_2 \cdot 2MeNO_2$ with the adopted numbering scheme. Displacement ellipsoids are drawn at 50% probability. Hydrogen atoms (except those on the macrocyclic N-donor), BF_4^- counteranions, and cocrystallized solvent molecules have been omitted for clarity. Cu(1)−N(3) = 1.967(4) Å, Cu(1)−O(1) = 1.920(3) Å, N(3)−Cu(1)−O(1) = 84.73(15)°, N(3^{i})−Cu(1)−O(1) = 95.27(15)°, N(3)−Cu(1)−N(3^{i}) = 180°, N(2)H(2)···N(1) = 1.98(6) Å, N(2)···N(1) = 2.824(6) Å, N(2)−H(2)···N(1) 159(5)°; i = 1 − *x*, 1 − *y*, −*z*.

to measure the solution magnetic moment of the complex by Evans' method.[46] It was found to be 4.18 μ_B, indicating the presence of three independent Cu^{II} centers in the complex (μ = 3.87 μ_B, S = 3/2). The serendipity of the reaction affording the cation $[Cu_3(5\text{-Cl-8-HDQH}_{-1})(\mathbf{L}^6\mathrm{H}_{-1})_2]^{3+}$ did not allow an investigation of the mechanism leading to its formation, but the crystal structure of this complex clearly shows the deprotonation of the hydroxyl group of $\mathbf{L}^6$ upon coordination to a metal center and the inability of the hydroxyquinoline moiety of $\mathbf{L}^6$ to coordinate via both its donor atoms in a 1:1 complex.

(46) Schubert, E. M. *J. Chem. Educ.* **1992**, *69*, 62.

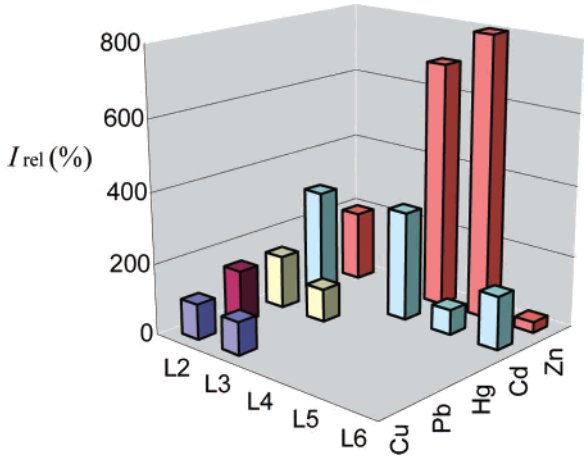

Figure 11. Effects [I_{rel} (%) = I/I_0] on the fluorescence intensity of $\mathbf{L^2}$, $\mathbf{L^3}$, $\mathbf{L^4}$ (MeCN/H_2O 4:1 v/v), $\mathbf{L^5}$, and $\mathbf{L^6}$ ((MeCN/H_2O 1:1 v/v), upon addition of Cu^{II}, Zn^{II}, Cd^{II}, Hg^{II}, or Pb^{II} (1 equiv). In the case of $\mathbf{L^3}$, for which an ON−OFF effect was observed upon addition of Cd^{II} or Zn^{II}, 100 − I_{rel} (%) is reported in the histogram. I_0 corresponds to the emission intensity of $\mathbf{L^2}$, $\mathbf{L^3}$, and $\mathbf{L^4}$ in the absence of metal ions.

The complexation reaction of $\mathbf{L^6}$ with $Cu(BF_4)_2 \cdot H_2O$ (in a 1:2 molar ratio in $MeNO_2$), followed by diffusion of Et_2O vapor into the reaction mixture, yielded single crystals of the complex $[Cu(\mathbf{L^6})_2](BF_4)_2 \cdot 2MeNO_2$. An X-ray diffraction analysis showed the metal center coordinated in a square planar geometry by the two deprotonated and trans bidentate hydroxyquinoline moieties from two $\mathbf{L^6}$ molecules (Figure 10). The two macrocyclic units are not involved in metal coordination, but in each, the aliphatic N-donor is protonated to give a NH···N [N(2)H(2)···N(1) = 1.98(6) Å, N(2)···N(1) = 2.824(6) Å, N(2)−H(2)···N(1) 159(5)°] hydrogen bond that presumably determines the observed folded conformation of the macrocyclic framework. This structure nicely supports the results from the potentiometric measurements (at least in the case of Zn^{II}) and indicates a high binding affinity of the $(5\text{-Cl-8-HDQH}_{-1})^{-1}$ moiety of $\mathbf{L^6}$ for the metal ions under investigation in either MeCN or MeCN/H_2O (1:1 v/v) mixtures, which may lead to "extraction" of the metal ion from the macrocyclic cavity in 1:1 complexes and formation of 1:2 metal-to-ligand complexes.

Conclusions

A great number of conjugated fluorescent chemosensors described in the literature contain polyoxa, polyaza, and oxaaza macrocycles as receptor units, but there are only a few reports of fluorescent chemosensors containing thia macrocycles, which are therefore suitable for the detection of "soft" metal ions.[24,26,47] We have described herein the synthesis and the coordination properties toward the "borderline" and soft metal ions Cu^{II}, Zn^{II}, Cd^{II}, Hg^{II}, and Pb^{II} of two new fluorescent chemosensors, $\mathbf{L^5}$ and $\mathbf{L^6}$ which incorporate the pyridine-based N_2S_2-donating 12-membered macrocycle $\mathbf{L^1}$ as a receptor unit. The optical response of these two ligands toward the same set of metal ions were investigated in MeCN/H_2O (1:1 v/v) solutions. Interestingly, $\mathbf{L^5}$ and $\mathbf{L^6}$ exhibited specificity toward Zn^{II} and Cd^{II}, respectively, over the other metal ions considered. These results are quite remarkable when compared to those previously obtained, in a similar solvent mixture (MeCN/H_2O, 4:1 v/v), for three other derivatives of $\mathbf{L^1}$ functionalized with different fluorogenic pendent arms, $\mathbf{L^2}$−$\mathbf{L^4}$, (Figure 11). In fact, while with $\mathbf{L^2}$ no specific changes in the fluorescence emission are observed upon interaction with the metal ions considered, with $\mathbf{L^3}$ and $\mathbf{L^4}$ the presence of coordinatively active fluorogenic fragments influences the specificity of the guest binding event because the former responds with the same efficiency only to the presence of Hg^{II} or Cu^{II} and the latter only to the presence of Cd^{II} or Zn^{II} with a preference twice as much for Zn^{II}. With $\mathbf{L^5}$ and $\mathbf{L^6}$, which are very similar to $\mathbf{L^4}$ from a structural point of view, we observe a much higher specificity of the former toward Zn^{II} and of the latter toward Cd^{II}. These results clearly indicate a synergic cooperation between the receptor and signaling units in determination of the substrate-specific response by a fluorescent chemosensor, although at this stage it is rather difficult to explain the role of the coordination of the fluorogenic fragment on the sensor specificity and to draw structural/specificity relationships. Therefore, in the search for a substrate selectivity and specificity, the common strategy of changing the receptor unit to discover the one with the best binding properties can be efficiently paralleled with the alternative strategy of keeping the receptor unit invariant and changing the signaling one. This last strategy might also offer some advantages from a synthetic point of view.

Acknowledgment. We thank the Ministero Italiano dell'Università e della ricerca Scientifica e Tecnologica (MIUR) for funding of Varian Cary Eclipse fluorescence spectrophotometer. We thank EPSRC (U.K.) for the provision of X-ray diffractometers.

Supporting Information Available: Crystallographic data in CIF format. This material is available free of charge via Internet at http//pubs.acs.org.

IC070169E

(47) (a) Tamayo, A.; Lodeiro, C.; Escriche, L.; Casabó, J.; Covelo, B.; González, P. *Inorg. Chem.* **2005**, *44*, 8105. (b) Tamayo, A.; Escriche, L.; Casabó, J.; Covalo, B.; Lodeiro, C. *Eur. J. Inorg. Chem.* **2006**, 2997.